THE ARCHIVE OF MECHANICAL ENGINEERING

VOL. LIV 2007 Number 1

DOI: 10.24425/ame.2007.131543

Key words: pipelay spread, dynamics, modelling, rigid finite element method

MAREK SZCZOTKA [*], *STANISŁAW WOJCIECH* [**], *ANDRZEJ MACZYŃSKI* [***]

MATHEMATICAL MODEL OF A PIPELAY SPREAD

The paper presents the mathematical model of a pipelay spread. In the model, elasto-plastic deflections of the pipe, its large deformations and contact problems are considered. The modification of the rigid finite element method (REFM) is used to discretise the pipe. The problem is analyzed in two stages. First, the quasi-static problem is considered. The tip of the pipe is pulled from the reel to the tensioner. Then, dynamic analysis (during ordinary work) of the pipelay spread is carried out. Some results of numerical calculations are presented.

1. Introduction

Advancing exploration of seas and oceans use laying pipes (for oil and gas), telecommunications cables etc. on sea bottoms. The conditions for such operations are very difficult due to high waves. Usually, special purpose vessels equipped with a reel on which the pipe (or cable) is reeled, and suitable laying devices are used. The first to use a buoyant drum for laying steel pipes were the Allies in 1944, during the invasion on France. Fig. 1 shows a contemporary buoyant drum used by the Dutch in constructing anti-storm dams. For some time, past reels have also been installed on ships, however, different techniques of laying pipes are used. Fig. 2 shows a solution applied by Hyundai and Fig. 3 by Natural Pipelay Limited.

The subject of the paper is a mathematical model of a pipelay spread presented in Fig. 4. The pipelay spread comprises a main reel and a lay ramp. It can handle both rigid and flexible pipes to up 18". The ramp has

[*] *Axess Technology AS, Oscar Hanssens vei 5, 6402 Molde, Norway; E-mail: marek.szczotka@axtech.no*

[**] *Faculty of Mechanical Engineering and Information Sciences, University of Bielsko-Biała; Willowa 2, 43-309 Bielsko-Biała, Poland; E-mail: swojciech@ath.bielsko.pl*

[***] *Faculty of Mechanical Engineering and Information Sciences, University of Bielsko-Biała; Willowa 2, 43-309 Bielsko-Biała, Poland; E-mail: amaczynski@ath.bielsko.pl*

a tensioner, whose role is to straighten and forward the pipe unreeled from the reel. The diameter of the reel is about 25 m and up to several kilometers of a pipe (depending on its diameter) may be reeled on it. In spite of the reel's large radius, reeling pipes of greater diameters requires their plastic deformation. After the ship has set off to the sea, the end of the pipe is put into the tensioner. The tensioner straightens and forwards the pipe at a velocity equal to that of the ship. To ensure a stable motion of the reel (weighing up to 2500 T), there are fences on its circumference connected with servomotors that ensure a moment balancing forces in the tensioner. A ship equipped with a pipelay spread of this type can lay up to twenty kilometers of the pipe a day. Application of such devices in real conditions shows that, when waves are huge and the ship swings vigorously, large dynamic forces emerge in the circuit, and they cause accelerations and decelerations in the rotational motion of the reel, which disturb the operation of the device. It may be dangerous for service and may lead to damage or breach of the pipe.

Fig. 1. Buoyant drum used on the Oosterscheldt Project

Fig. 2. Hyundai pipelay spread

Fig. 3. Natural Pipelay Limited pipelay spread

Fig. 4. Pipelay spread with a lay ramp and a tensioner

The problems concerning laid or towed cables have been considered in [Srivastava S.K., Ganapathy C., 1998], [Croll J.G.A., 2000], [Feng, Z. Allen, R., 2004], however, these publications describe phenomena in the cable already leaving the pipelay spread. The authors have not found any papers concerning the analysis of the pipelay spread.

In the paper, a simplified model of the device is presented which allows for a preliminary analysis of phenomena occurring when it operates in the conditions of high waves on the sea.

2. Analysis of the problem

For the analysis, the following assumptions are made:

- Only planar models are considered. This assumption not only simplifies the problem, but it also follows on the experience, which shows that most important disturbances of the reel motion are caused by a pitch angle when the sea is weaving.
- The tensioner is treated as a non-deformable rigid body.
- Elasto-plastic deflections of the pipe are considered. It is an important property of the system which influences the pipe laying process.
- Large deformations of the pipe should be also taken into account. This leads to a nonlinear problem.
- Flexibility of the pipe is considered by means of the modification of the rigid finite element method (RFEM) [Wittbrodt E. et al., 2006]. That is a method of discretisation, which gives good results of calculations and requires relatively short calculation time. The idea of the method is to discretise flexible links into rigid elements (*ref*) containing inertial features of bodies; these rigid elements are connected by massless and non-dimensional spring-plastic elements (*spe*). In this method, large deformations and plasticity of the pipe can be taken into considerations.

The problem is analyzed in two stages. First, the quasi-static problem is considered. The pipe is moved from the initial position presented in Fig. 5a, when the pipe is totally coiled on the reel, to the position from Fig. 5b, when its tip is put into the tensioner and tighten by the tensioner force $T_{\max}$.

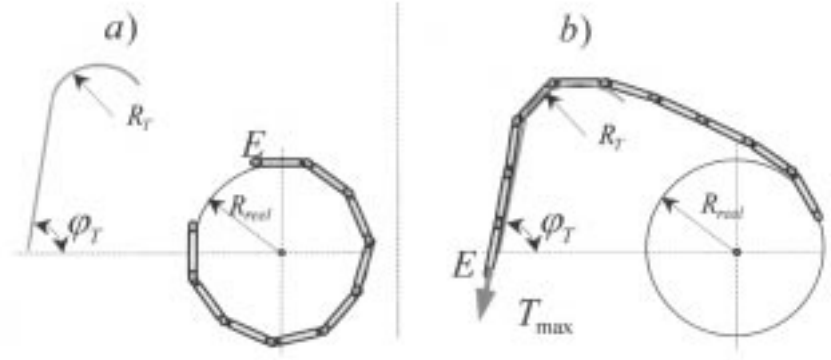

Fig. 5. Initial and final positions of pipe elements for the quasi-static problem a) initial position b) final position

In the initial position, all spring-plastic elements (*spe*) are assumed to be deformed. Then, the pipe tip E is moved to the final position. It is assumed that point E moves along a tangential to the given trajectory, until it achieves

point T_N (tensioner). When pipe tip E is in the tensioner, the pipe is tensioned up to maximal (or nominal) force $T_{\max}$.

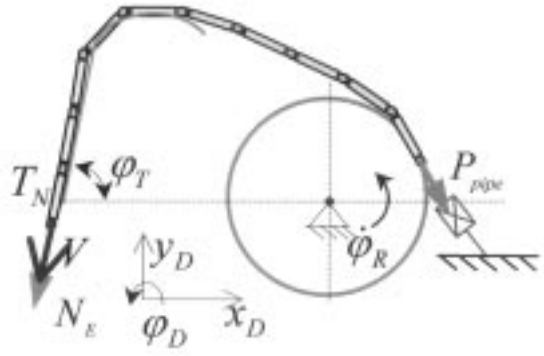

Fig. 6. Dynamic phase of pipe-reel motion

Then, dynamic analysis is carried out. Having solved the quasi-static task, we are able to define initial conditions for dynamic problem (Fig. 6). In this case, the pipe tip moves with constant velocity V in the tensioner, while the vessel motion is caused by sea waves. The waves are defined by harmonic functions $x_D(t)$, $y_D(t)$, $\varphi_D(t)$.

3. Quasi-static analysis of the tensioner-pipe-reel system

In this section, the following problems are discussed:

- transportation of the pipe from the reel to the tensioner,
- increase of the tension force from the value calculated in the previous task up to nominal (maximal) value,
- quasi-static analysis.

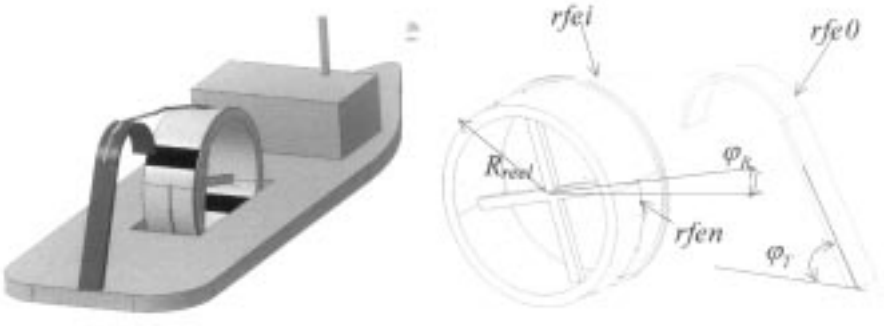

Fig. 7. Model of the pipe laying system

Fig. 7 presents a scheme of the vessel with the reel and the tensioner and pipe divided into rigid finite elements (*rfes*), numbered from *n* to *0*.

3.1. Moving the pipe from reel to the tensioner – TASK1

In this task, the tip of the pipe is moved according to a specific trajectory, which depends on the system geometry (reel effective diameter, tensioner angle and shape of its head etc.). We assume that initial part of this trajectory is a straight line. Reel angle φ_R changes from to a final value φ_{Tend}, with step $\Delta\varphi_T$. Constant force S_E, tangential to the assumed trajectory (Fig. 8), act at point E (tip of the pipe). When friction is omitted, the reaction N_E normal to the trajectory should be taken into account.

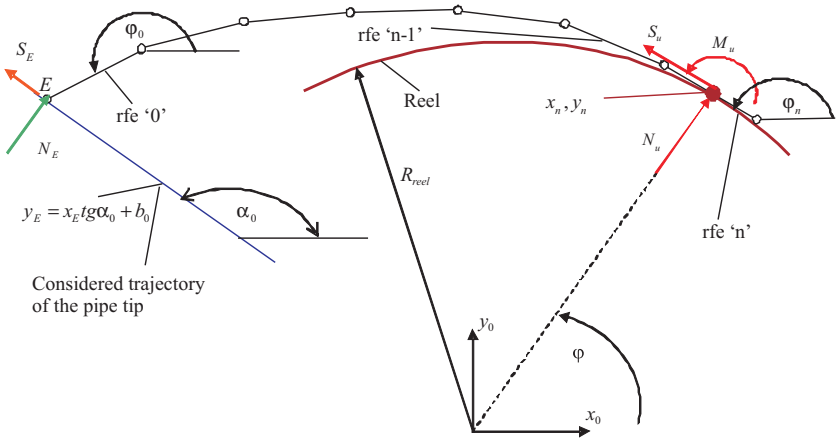

Fig. 8. Designations used for TASK1

Below, the static equilibrium of the pipe's finite elements are discussed.

Equilibrium of the *rfe i* ($i = 1, ..., n-1$)

The system of forces and torques acting on the *rfe i* is presented in Fig. 9.

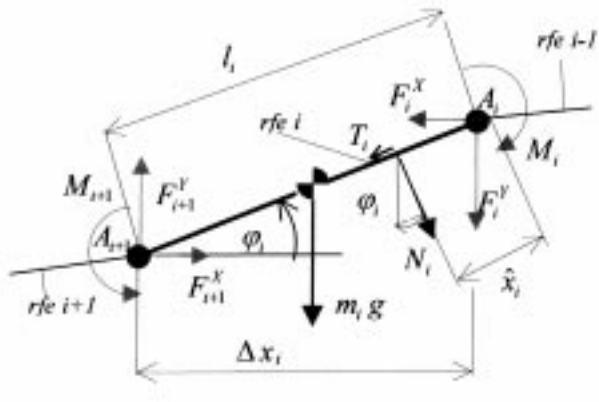

Fig. 9. System of forces and moments acting on *rfe i*

The equations of static equilibrium are formulated as follows:

$$\begin{aligned}
&\sum P_{ix} = F_{i+1}^X - F_i^X + N_i \sin\varphi_i - T_i \cos\varphi_i = 0,\\
&\sum P_{iy} = F_{i+1}^Y - F_i^Y - m_i g - N_i \cos\varphi_i - T_i \sin\varphi_i = 0,\\
&\sum M_i = M_{i+1} - M_i + F_i^X \cdot \Delta y_i - F_i^Y \cdot \Delta x_i - m_i g \frac{\Delta x_i}{2} - N_i (l_i - \hat{x}_i) = 0,
\end{aligned} \tag{1}$$

where:
$\Delta x_i = l_i \cdot \cos\varphi_i$, $\Delta y_i = l_i \cdot \sin\varphi_i$,
N_i, T_i are the reel or the tensioner head's reactions acting on *rfe i*.

Equilibrium of *rfe 0* and *rfe n*

The system of forces acting on *rfe 0* and *ref n* is presented in Fig. 10a and 10b, respectively. The following notations are used: N_E – force normal to the trajectory at point $\langle x_0, y_0\rangle$, S_E – assumed force tangential to the trajectory, ψ – angle denoted as in Fig. 10a, S_u, N_u – components of constraint force, M_u – constraint moment. For these *refs*, equations of static equilibrium are similar to (1).

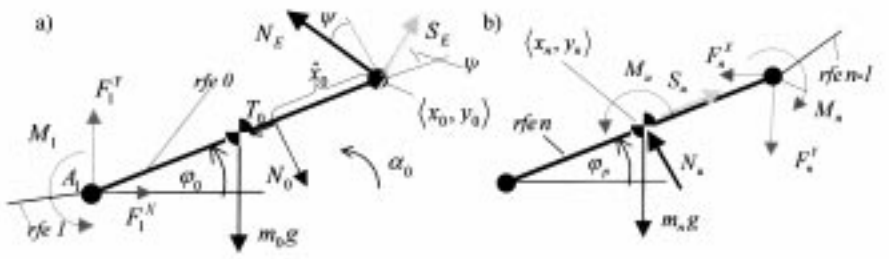

Fig. 10. System of forces and moments acting on: a) *rfe 0* b) *ref n*

Using these equations, we can calculate joint forces F_i^x, F_i^y for $i = 1, ..., n$, and later torques (moments) $M_i = M_i(F_i^x, F_i^y)$.

Torques M_i must be equal to moments caused by deformations of spring-plastic elements *spe 1* ÷ *n*:

$$M_i^{sp} = M_i^{sp}\left(\varphi_{i-1},\ \varphi_i,\ \Delta\varphi_i^0\right) \tag{2}$$

where $\Delta\varphi_i^0$ is an initial angle of plastic deformation $\varphi_{i-1} - \varphi_i$.

Thus, the following system of n algebraic nonlinear equations is obtained:

$$M_i^{sp} - M_i = 0, \quad i = 1,\ 2,\ ...,\ n \tag{3}$$

Angles φ_0, ..., φ_{n-1} and normal reaction N_E at the tip of the pipe are unknown variables. The number of unknowns is $n+1$, while formulae (3) form

only n equations. An additional equation can be formulated by taking into account the constraint equation. According to the assumption that point E (the tip of pipe) moves tangentially to the given trajectory, the following equation can be written:

$$y_E = f_T(x_E) \tag{4}$$

where f_T is a function that describes the trajectory of point E.

In the case when point E moves as in Fig. 8, the equation (4) takes the form:

$$y_E = x_E tg\alpha_0 + b_0. \tag{5}$$

Having defined following vector of unknowns:

$$\mathbf{X} = [\varphi_0,\ \varphi_1, ...,\ \varphi_{n-1},\ N_E]^T \tag{6}$$

one can write equations (3) and (4) as:

$$f(\mathbf{X}) = 0 \tag{7}$$

Equations (7) form a system of $n+1$ nonlinear algebraic equations with $n+1$ unknown coordinates of vector $\mathbf{X}$ defined in (6). One of the most numerically effective methods, which can be applied in order to solve such a system, is the Newton method [Ralson A., 1971].

3.2. Contact forces

Up to now we have assumed that contact forces N_i, T_i between the pipe and the reel or tensioner head are known. The both cases are similar in description, so the general problem, in which forces between some rigid finite element and the reel (the tensioner) are defined, is presented in Fig. 11.

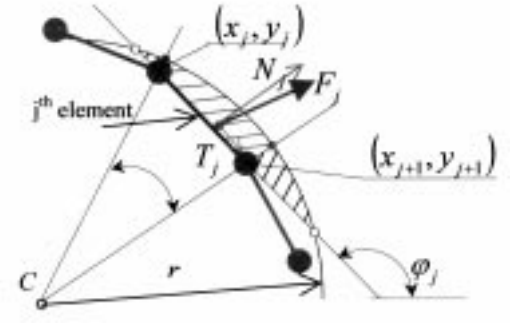

Fig. 11. Model of contact forces N_j, T_j between *rfe j* and the reel (the tensioner)

In the case when RFE method is applied to discretise the pipe, a specific way in which *rfe* deflect the reel (the tensioner) has to be taken into account. Let us consider the general case of a ring with radius r and radial flexibility. Its center is denoted by (x_C, y_C) as in Fig. 12. The *rfe j* lies on the axis defined by the equation:

$$y = a_j x + b_j, \tag{8}$$

where $a_j = \dfrac{y_j - y_{j+1}}{x_j - x_{j+1}}$, $b_j = y_j - a_j x_j$.

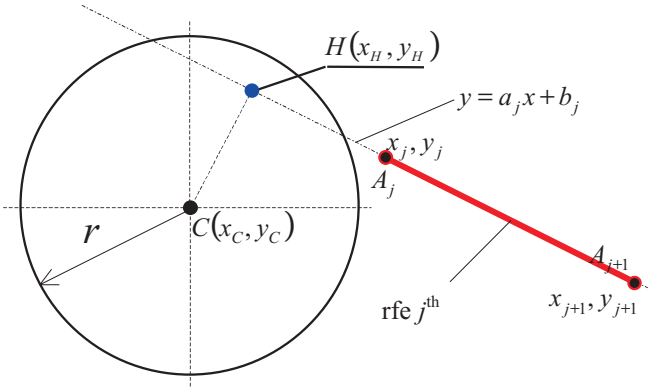

Fig. 12. Flexible ring and *rfe j*

The coordinates of point H can be calculated according to the following formulae:

$$x_H = \frac{a_j\left(b_j^H - b_j\right)}{1 + a_j^2}, \tag{9.1}$$

$$y_H = a_j \cdot x_H + b_j. \tag{9.2}$$

The distance CH has an influence on contact phenomenon:

$$CH = \left|\overline{CH}\right|. \tag{10}$$

If $CH \geqslant r$, there is no contact between the ring and *rfe j*. If $CH < r$, the contact is possible.
We define the following:

$$d_j = \left|\overline{CA_j}\right|, \tag{11.1}$$

$$d_{j+1} = \left|\overline{CA_{j+1}}\right|. \tag{11.2}$$

If $d_j > r$ and $d_{j+1} > r$ and $H \notin \overline{A_j A_{j+1}}$, then there is no contact between the ring and *rfe j*.
The contact occurs when:

$$CH < r, \tag{12}$$

and when one of the following conditions is fulfilled:

$$d_j \geqslant r \text{ and } d_{j+1} \geqslant r \text{ and } H \in \overline{A_j A_{j+1}}, \tag{13.1}$$

or

$$d_j \geqslant r \text{ and } d_{j+1} < r, \tag{13.2}$$

or

$$d_j < r \text{ and } d_{j+1} \geqslant r, \tag{13.3}$$

or

$$d_j < r \text{ and } d_{j+1} < r, \tag{13.4}$$

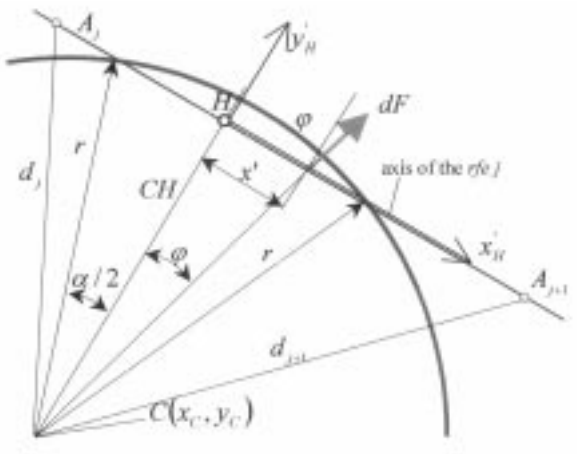

Fig. 13. Case when $d_j \geqslant r$ and $d_{j+1} > r$

If the position of point A (Fig. 13) that belongs to $\overline{A_j A_{j+1}}$ is defined by x' in the local coordinate system $x'_H y'_H$, then the elementary contact force caused by radial ring deflection dF can be calculated as:

$$d\mathbf{F} = dx' \cdot c\,(\Delta) \cdot \begin{bmatrix} \sin\varphi \\ \cos\varphi \end{bmatrix} \tag{14}$$

where $\varphi = arctg\left(\frac{x'}{CH}\right)$, $\Delta = r - \sqrt{x'^2 + CH^2}$ – is the ring deflection.
Let us assume that x'_1 and x'_2 are the beginning and the end of deflection, respectively. We can then calculate the forces caused by them:

$$F_{x'} = \int_{x'_1}^{x'_2} c\,(\Delta) \sin\varphi dx' \tag{15.1}$$

$$F_{y'} = \int_{x'_1}^{x'_2} c\,(\Delta) \cos\varphi dx' \tag{15.2}$$

$$x'_F = \frac{1}{F_{y'}} \int_{x'_1}^{x'_2} c\,(\Delta)\, x' \cos\varphi dx' \tag{15.3}$$

where:
$F_{x'}, F_{y'}$ are reaction forces,
x'_F is the position of the reaction force in the local coordinate system (x'_H, y'_H).
Values x'_1, x'_2 for cases (13.1) – (13.4) must be defined, and then equations (15) can be calculated.

Here we discuss only the case described by Eq. (13.1). The other cases can be considered in the same way. The following can be obtained (Fig. 13):

$$x'_1 = -\sqrt{r^2 - CH^2}, \tag{16.1}$$

$$x'_2 = +\sqrt{r^2 - CH^2}, \tag{16.2}$$

$$F = F_{y'}, \tag{16.3}$$

$$F_{x'} = 0, \tag{16.4}$$

$$x'_F = 0. \tag{16.5}$$

Equation (16.5) implies that

$$x_j = \left|A_j H\right|, \tag{17}$$

where x_j is the distance from point A_j to the reaction.

Integrals (15) are calculated using the Gauss formulae of the third order [Legras J., 1974].

3.3. Stiffness characteristics

When linear characteristic of the contact force is applied, the gradient of force F_i is not continuous, and one may encounter some numerical problems with solution of equations (7). Thus, it is assumed that the stiffness characteristic of the ring is defined in Fig. 14.

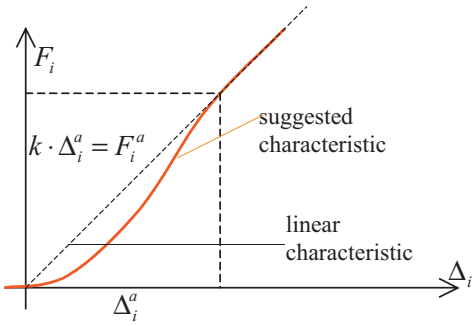

Fig. 14. Assumed characteristic of radial stiffness of ring

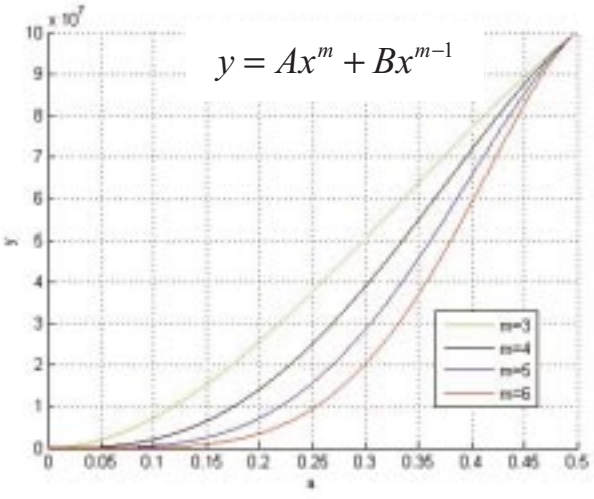

Fig. 15. Examples of ring stiffness characteristics

The function describing force F_i according to Fig. 14 can be defined as follows:

$$F_i = \begin{cases} 0 & \Delta_i < 0 \\ A \cdot \Delta_i^m + B \cdot \Delta_i^{m-1} & \text{when} \quad 0 < \Delta_i < \Delta_i^a \\ k \cdot \Delta_i & \Delta_i^a < \Delta_i \end{cases} \tag{18}$$

where:
$m > 2$,
Δ_i^a, k – assumed constants.
Some examples of such characteristics are presented in Fig. 15. In further calculations, $m = 3$ is assumed.

3.4. The parameters of spring-plastic elements

One of the most important parameters used in the model are those concerning material elastoplastic properties. For the problem analyzed, it is necessary to take into account plasticity and plastic deformations of the pipe. When the pipe moves from the reel to the tensioner, its shape is determined by the system of forces and by actual permanent plastic deformation. The assumed elastoplastic characteristic of the pipe is presented in Fig. 16.

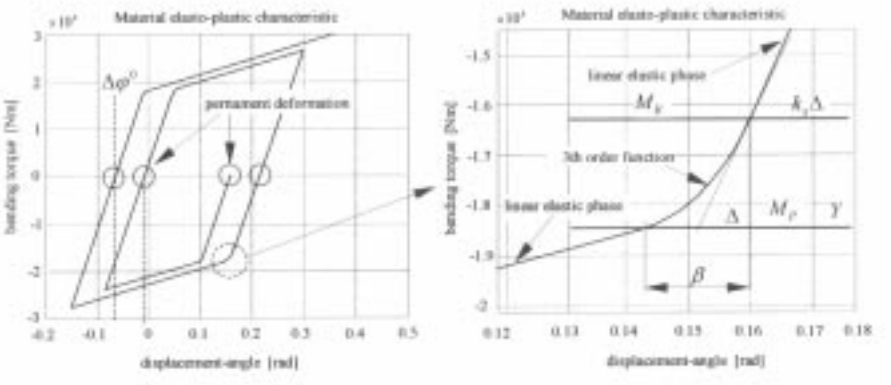

Fig. 16. Elasto-plastic characteristic of material a) assumed shape of the characteristic b) smooth function between elastic and plastic phases

It is assumed, that the stiffness coefficient is greater than 0 in the plastic phase of the characteristic:

$$k_{pl}^{(i)} = \kappa \cdot k_s^{(i)}, \tag{19}$$

where:
κ – coefficient (eg. $\kappa = 0.05 \div 0.1$),
$k_s^{(i)} = \dfrac{E \cdot J_p}{l_i}$ – elastic stiffness of the *spe i*,

E – Young's modulus,
J_p – moment of inertia of the pipe's cross-section,
l_i – length of element i.
The actual deformation of *spe i* is described as follow:

$$\Delta\varphi_i = \varphi_{i-1} - \varphi_i - \Delta\varphi_i^0, \tag{20}$$

where $\Delta\varphi_i^0$ – initial deformation (with zero bending torque).

Third order functions have been used for smoothing of elastoplastic phase in order to improve the stability of calculations. In Fig. 16, the following notations are used: M_p – bending moment corresponding to yield point, $M_E = \alpha M_p$ – maximum elastic torque in the linear range of elastic phase, $\Delta = \dfrac{M_p - M_s}{k_s}$, $\beta = \varepsilon \cdot \Delta$ – length of the third order transmission phase. Parameters α and ε are selected by the user. We assumed that $\alpha = 0.9$ and $\varepsilon = 3$.

3.5. The nominal tension force – TASK2

The second task provides the method that allows us to obtain a nominal tension force (force that is applied to the pipe in the tensioner). The result of the TASK1 forms the initial configuration for TASK2.

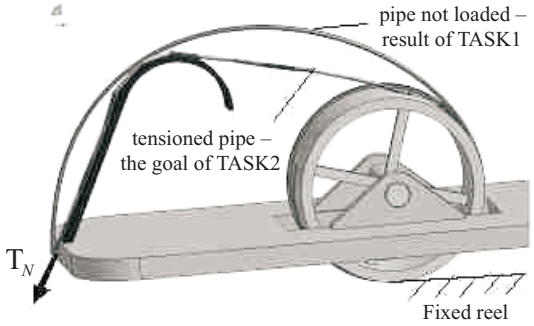

Fig. 17. The goal of TASK2

The problem to be solved is:
Starting from $T_N = T_0$ increase the tension force $T_N = T_N + \Delta T_N$ until $T_N = T_{N_{nom}}$. Additionally, the angle of rotation of *ref 0* should agree with tensioner arm angle when tension force $T_N = T_{N_{non}}$.
Fig. 18 shows forces acting on *rfe 0* in the tensioner. The angle of the tensioner arm is denoted as φ_T.
Let us denote:

$$\varphi_0' = \varphi_0 - \pi. \tag{21}$$

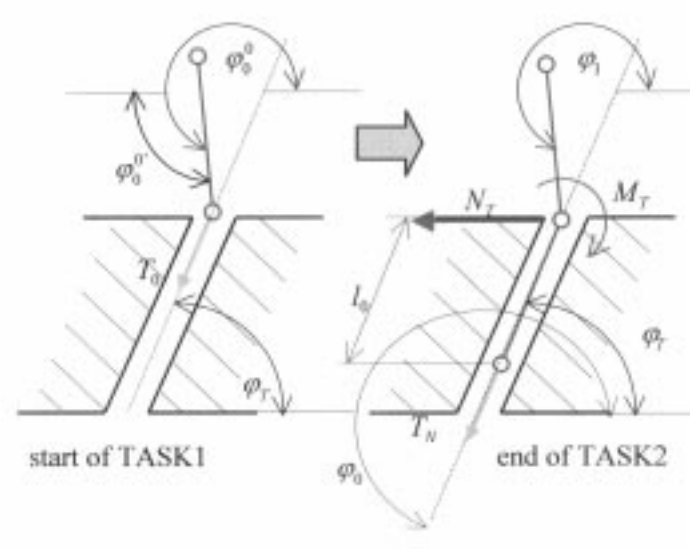

Fig. 18. System of forces acting on *ref 0*

Kinematic input function $\varphi_0' = f(T_N)$ presented in Fig. 19 has been used in order to ensure that the angle φ_0 of *ref 0* will be $\varphi_0 = \varphi_T + \pi$ when $T_N = T_{Nnom}$.

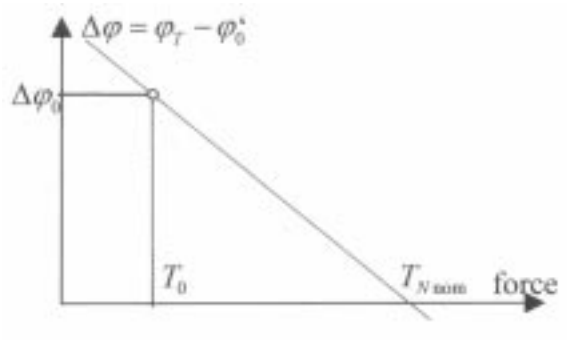

Fig. 19. Kinamatic input function of angle φ_0

When we calculate $\Delta\varphi_0 = \varphi_T - \varphi_0^{0'}$, the angle φ_0' is defined by the following function:

$$f(x) = \frac{\varphi_T - \varphi_0'}{T_0 - T_{Nnom}} x - T_{Nnom} \frac{\varphi_T - \varphi_0'}{T_0 - T_{Nnom}}, \tag{22}$$

where:
$x = T_0 + \Delta_F$, $x \in \langle T_0, T_{Nnom} \rangle$,
Δ_F – step of tension force increasing.

The moment M_T, which can be calculated from additional constraint equation (because the angle φ_0 is known), have to be applied to the element *0*.

3.6. Quasi-static analysis

Quasi-static analysis is carried out when dynamic forces are neglected during the analysis of motion of the system.

For the analysis, it is assumed that the reel rotates with an angular velocity determined by the linear velocity of the pipe tip in the tensioner as follows:

$$\omega = \dot{\varphi}_{reel} = \frac{V_T}{R_{reel}} \tag{23}$$

where:
φ_{reel} – rotation angle of the reel,
R_{reel} – radius of the reel.
This means that velocities of *ref 0* and *refs* which are in contact with the reel are known. System of equations of static equilibrium is similar to (7), but the vector of unknowns is defined as:

$$\mathbf{X} = \left[\varphi_0,\ \varphi_1, ...,\ \varphi_{n-1},\ N_E, S_{pipe}\right]^T \tag{24}$$

and two additional constraint equations are formulated.

The forces acting on the reel can be obtained as the result of the analysis,. Therefore, the force in the tensioner is calculated in order to define the force S_{pipe} – acting on the reel (from the pipe side). Then, the hydraulic friction force S_H, related to constant velocities of the reel and the pipe (Fig. 20), is also calculated. As a consequence, force $S_E = T_N$ can be considered as a new unknown value, which is determined when the equations of the quasi-static problem are solved.

4. Quasi-dynamic model

In this model, only dynamic equation of reel rotational motion is considered (Fig. 20) without the equations of pipe elements (*refs*). The equation of the reel motion is integrated when the shape of the pipe and forces acting on the reel are calculated in the quasi-static analysis performed in each integration step of the reel dynamic equation. This allows us to simulate the motion of the pipe.
The equation of motion of the reel can be written in the following form:

$$I_{reel}\left(\ddot{\varphi}_{reel} + \ddot{\varphi}_D\right) = \left(S_{pipe} - S_H\right) R_{reel} \tag{25}$$

where:
I_{reel} – moment of inertia of the reel,
φ_D – angle of rotation of the vessel (pitch angle).

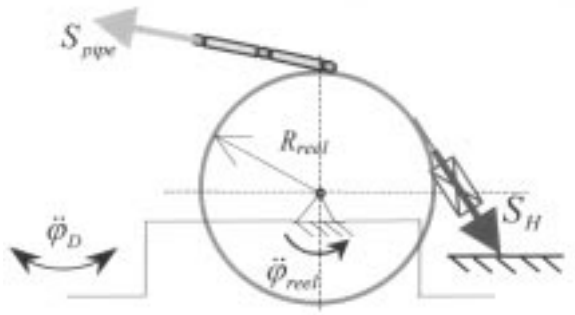

Fig. 20. System of forces acting on reel

The Runge-Kutta method of fourth order with a fixed step size is used to solve equation (25). Force S_{pipe} is calculated during nonlinear static sub-analysis, which is performed at every integration step of (25). Additionally, the analysis of each sub-analysis requires the number of sub-steps to be carried out where the position and deformation of the pipe are calculated. The models and algorithms used in the static analysis are derived above. The algorithm applied is presented in Fig. 21.

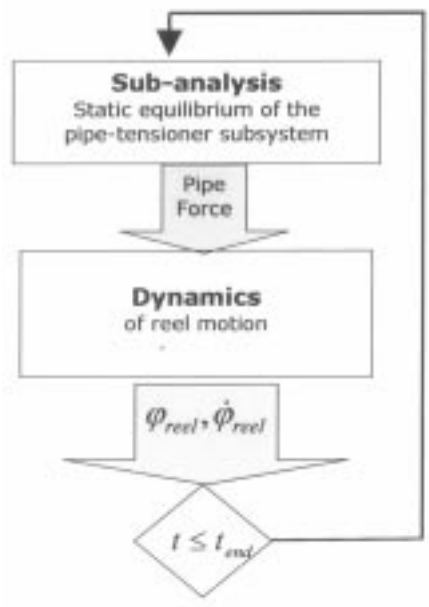

Fig. 21. Loop quasi-dynamic analysis

This model allows us to simulate dynamics of the reel caused by:

- force S_E acting on the pipe tip,
- wavy motion of the vessel φ_D,
- hydraulic force S_H (different input functions can be modelled).

5. Numerical calculations. Conclusions

Calculations have been carried out for the following parameters: pipe size 12", reel effective radius R_{reel} = 12.212 m, reel moment of inertia I_{reel} = 2.66e8 kg*m^2. The sea conditions corresponding to waves are described by the following function:

$$\varphi_D = A \cos \frac{2\pi}{T} t \tag{26}$$

and parameters are given in Table 1.

Table 1.

Parameters of sea waves

S1	$A = 0$	calm sea
S2	$A = 4.4°$, $T = 6.9$ [sec]	waves with amplitude of 3 [m]
S3	$A = 11.4°$, $T = 9$ [sec]	waves with amplitude of 8 [m]

Time courses of the reel angular velocity and acceleration, as well as time courses of forces $S_E = T_N$ and S_{pipe} are presented in Fig. 22, 23 and 24.

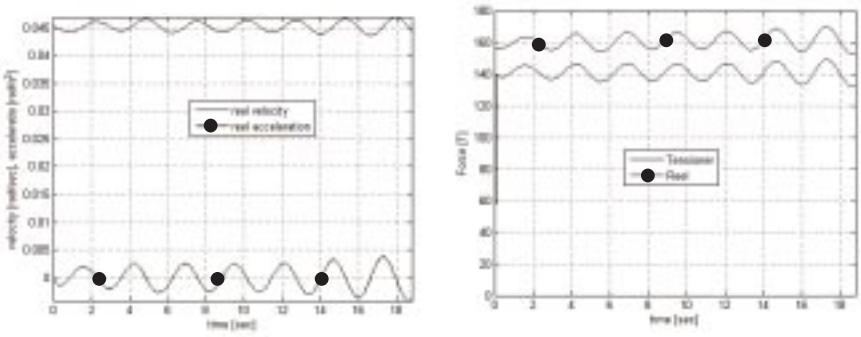

Fig. 22. Results of calculations – S1

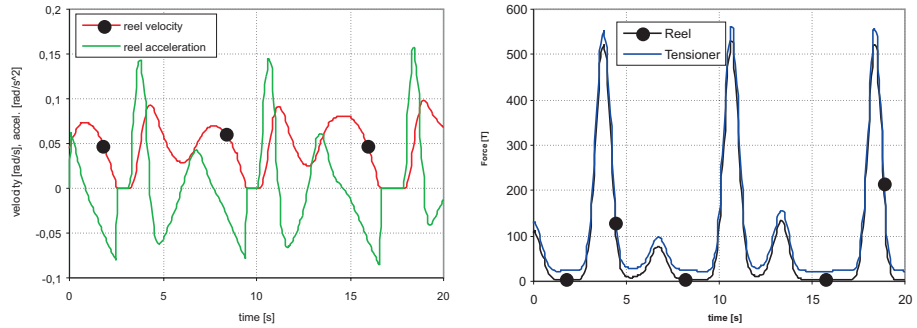

Fig. 23. Results of calculations – S2

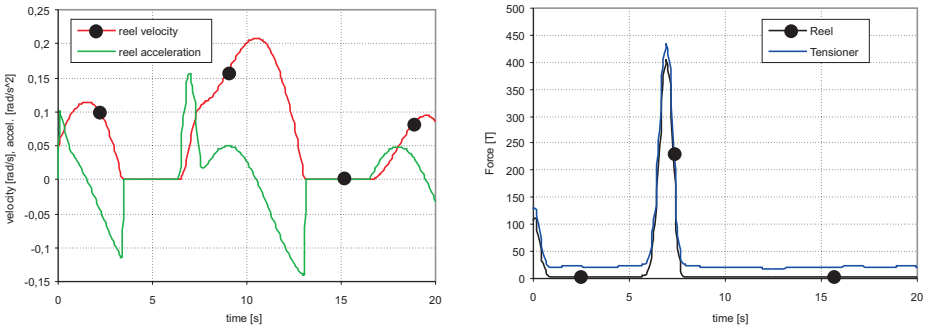

Fig. 24. Results of calculations – S3

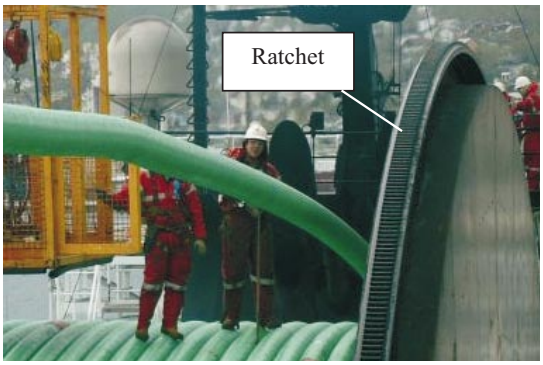

Fig. 25. Ratchet

It can be seen that when the sea is calm reel angular velocity and acceleration, as well as forces, are almost constant. For wavy sea these courses are quite different. The velocity of the reel is not constant and, moreover, it may drop to 0. The reel is designed in such a way that there is no possibility of backward movement. This is due to a special ratchet mechanism (Fig. 25). It should be mentioned that the maximum dynamic forces S_E and S_{pipe} exceed

the nominal tension values up to 5 times. Furthermore, higher forces are obtained for smaller waves with higher frequency.

These results are consistent with engineering experience. Our present research is concerned with the problem – how to control the motion of the reel so that the force S_{pipe} is almost constant, regardless of sea conditions.

Manuscript received by Editorial Board, August 01, 2006;
final version, December 04, 2006.

REFERENCES

[1] Croll J. G. A.: Bending boundary layers in tensioned cables and rods. Applied Ocean Research Volume: 22, Issue: 4, August, 2000, pp. 241÷253.
[2] Feng Z., Allen R.: Evaluation of the effects of the communication cable on the dynamics of an underwater flight vehicle. Ocean Engineering Volume: 31, Issue: 8-9, June, 2004, pp. 1019÷1035.
[3] Legras J.: Praktyczne metody analizy numerycznej. WNT, Warszawa, 1974.
[4] Ralaon A.: Wstęp do analizy numerycznej. PWN, Warszawa, 1971.
[5] Srivastava S. K, Ganapathy C.: Experimental investigations on loop manoeuvre of underwater towed cable-array system, Ocean Engineering Volume: 25, Issue: 1, January, 1998, pp. 85÷102.
[6] Wittbrodt E., Adamiec-Wójcik I., Wojciech S.: Dynamics of flexible multibody systems. Springer, 2006.

Photos in Fig. 1–3 come from http://www.naturalay.com/ (date: 25.06.2006)
Photo in Fig. 4 comes from http://www.offshore-technology.com/projects/glider/glider3.html (date: 25.06.2006)
Photo in Fig. 25 comes from http://www.caithness.org/links/oil/photogallery/ (date: 25.06.2006)

Matematyczny model urządzenia do układania rur na dnie morza

Streszczenie

W pracy przedstawiono matematyczny model urządzenia do układania rur na dnie morza. W modelu uwzględniono sprężysto-plastyczne odkształcenie rury, jej duże odkształcenia oraz zjawiska kontaktowe. Do dyskretyzacji rury zastosowano zmodyfikowaną metodę sztywnych elementów skończonych. Analizę przeprowadzono w dwóch etapach. Najpierw rozważano zagadnienie quasi-statyczne przemieszczenia końca rury z bębna do napinacza. Następnie wykonano analizę dynamiczną pracy urządzenia w trakcie jego normalnej pracy. Zaprezentowano wybrane wyniki obliczeń numerycznych.